Article

Reassessment of the transport mechanism of the human zinc transporter SLC39A2

Marie Christine Franz, Jonai Pujol-Gimenez, Nicolas Montalbetti, Miguel Fernandez-Tenorio, Timothy R. DeGrado, Ernst Niggli, Michael F. Romero, and Matthias A. Hediger

Biochemistry, **Just Accepted Manuscript** • DOI: 10.1021/acs.biochem.8b00511 • Publication Date (Web): 23 May 2018

Reassessment of the transport mechanism of the human zinc transporter SLC39A2

Marie C. Franz[1, 4, #], Jonai Pujol-Giménez[1, #], Nicolas Montalbetti[1, 5)], Miguel Fernandez-Tenorio[2)],Timothy R. DeGrado[3)], Ernst Niggli[2)], Michael F. Romero[3)] and Matthias A. Hediger[1, *]

[#] **Both authors contributed equally to this work**

*** Corresponding Author:**

Matthias A. Hediger

Institute of Biochemistry and Molecular Medicine

University of Bern, Bühlstrasse 28

3012 Bern

Switzerland

Tel: +41 31 631 41 29

Email: Matthias.hediger@ibmm.unibe.ch

[1)] University of Bern, Institute of Biochemistry and Molecular Medicine and National Center of Competence in Research, NCCR TransCure, Bühlstrasse 28, 3012 Bern, Switzerland.

[2)] University of Bern, Department of Physiology, Buehlplatz 5, 3012 Bern, Switzerland

[3)] Mayo Clinic College of Medicine and Science, Department of Physiology and Biomedical Engineering, Mayo Clinic Joseph Building, Rochester, MN 55905, USA

[4)] Current address: CSL Behring, Wankdorfstrasse 10, 3014 Bern, Switzerland

[5)] Current address: University of Pittsburgh, Department of Medicine, 3550 Terrace Street, Pittsburgh, PA 15261, USA.

Abstract

The human zinc transporter SLC39A2, also known as ZIP2, was shown to mediate zinc transport that could be inhibited at pH values below 7.0 and stimulated by HCO_3^-, suggesting a Zn^{2+}/HCO_3^- cotransport mechanism (1). In contrast, recent experiments in our laboratory indicated that the functional activity of ZIP2 increases at acidic pH (2). The present study was therefore designed to reexamine the findings on the pH-dependence and to extend the functional characterization of ZIP2.

Our current results show that ZIP2-mediated transport is modulated by extracellular pH, but independent of the H^+ driving force. Also, in our experiments, ZIP2-mediated transport is not modulated by extracellular HCO_3^-. Moreover, high extracellular $[K^+]$, which induces depolarization, inhibited ZIP2-mediated transport, indicating that the transport mechanism is voltage-dependent.

We also show that ZIP2-mediates the uptake of Cd^{2+} (K_m~ 1.57 μM) in a pH-dependent manner (K_{H+} of ~66 nM). Cd^{2+} transport is inhibited by extracellular $[Zn^{2+}]$ (IC_{50}~ 0.32 μM), $[Cu^{2+}]$ (IC_{50}~ 1.81 μM) and to a lower extend by $[Co^{2+}]$, but not by $[Mn^{2+}]$ or $[Ba^{2+}]$. Fe^{2+} is not transported by ZIP2. Accordingly, the substrate selectivity of ZIP2 decreases in the order $Zn^{2+} > Cd^{2+} \geq Cu^{2+} > Co^{2+}$.

Altogether, we propose that ZIP2 is a facilitated divalent metal ion transporter that can be modulated by extracellular pH and membrane potential. Given that ZIP2 expression has been reported in acidic environments (3-5), we suggest that the herein described H^+-mediated regulatory mechanism might be important to determine the velocity and direction of the transport process.

Introduction

Zinc is an essential trace element for human nutrition and the second most abundant transition element after iron in living organisms. The importance of zinc becomes evident when looking at a recent bioinformatics analysis indicating that as much as 10% of the human proteome is potentially capable of binding zinc (6). Over 3000 different types of proteins require zinc as a key structural or catalytic component. Among them are transcription factors, signaling proteins, transport/storage proteins, zinc finger proteins and proteins involved in DNA repair, replication and translation (7). Whole body and cellular zinc homeostasis is being thoroughly regulated. Whereas systemic zinc intoxication is relatively rare, zinc deficiency is a widespread problem leading to growth retardation, cognitive impairment and immune dysfunction (8). Maintenance of mammalian zinc homeostasis is achieved by high-affinity zinc transport systems that are regulated by metal sensors (7). There are at least two different solute carrier (SLC) families of zinc transporters that control Zn^{2+} movement across membranes: 1) The SLC30 zinc transporter family, also known as ZnT family, that facilitate cellular efflux or uptake into intracellular compartments; and 2) the SLC39 family, also known as ZIP[1)] family that facilitates cellular uptake or efflux from intracellular compartments (9-12).

The mammalian SLC39/ZIP family consists of 14 members, which can be divided into four subfamilies based on sequence similarity. SLC39A2 (ZIP2) together with SLC39A1 (ZIP1) and SLC39A3 (ZIP3) comprises subfamily II. ZIP2 was originally cloned and characterized by Gaither and Eide in year 2000 (1). In this study, they showed that ZIP2-expressing K562 cells accumulated more $^{65}Zn^{2+}$ than parental cells, in a time-, temperature- and concentration-dependent manner. They found that ZIP2-dependent zinc transport was not dependent on ATP hydrolysis and neither on Na^+ or K^+ gradients. In their assay, ZIP2 was inhibited at acidic pH (pH < 7.0) and stimulated by 0.5 mM HCO_3^-. Thus, they proposed a Zn^{2+}/HCO_3^- cotransport mechanism. In the same study, expression of *ZIP2* mRNA was found to be generally low or negligible in human tissues and cultured cell lines, except in prostate and uterus (1), where it indeed could also be detected at the protein level (3). Cao *et al.* found *ZIP2* mRNA in peripheral blood mononuclear cells (PBMCs) and monocytes (13). In their study, zinc depletion in both cell lines triggered upregulation of *ZIP2* with concomitant downregulation of zinc-binding metallothioneins. Recently, Inoue *et al*. could detect ZIP2 in the epidermis of healthy human frozen skin samples (4). They discovered that ZIP2 was upregulated by differentiation induction of cultured keratinocytes. Interestingly, ZIP2 knockdown inhibited the differentiation of keratinocytes and consequently the formation of a 3D cultured epidermis. Several studies have linked the down-regulation of ZIP2 in prostatic tissue to decreased zinc levels in prostatic epithelial cells and to prostate cancer (3,14-18). Studies with ZIP2-KO

[1] ZIP, ZrT/Irt-like protein

mice did not reveal any specific phenotype. However, these mice were more susceptible to abnormal embryonic development due to zinc deficiency during pregnancy (19).

Recently, we published a screening assay that was established using the FLIPR Tetra high throughput microplate reader to identify specific modulators of ZIP2 as potential therapeutic hit or lead compounds (2). This assay is based on the use of a Ca^{2+}-sensitive dye, Calcium 5 (Molecular Devices), which, in addition to Ca^{2+}, binds Cd^{2+} with high affinity. Binding of either Ca^{2+} or Cd^{2+} to the dye induces emission of a fluorescent signal that can be monitored, allowing quantification of transport activity of proteins that mediate Cd^{2+} influx, such as ZIP2, which transports Cd^{2+} efficiently (1,2). In our laboratory, this assay has been successfully used to monitor the activity of a variety of Cd^{2+} transporting proteins such as the human divalent metal transporter DMT1 (SLC11A2) (20) or the epithelial calcium channel TRPV6 (21). Interestingly, during the development of the assay, we discovered discrepancies between our results on ZIP2 transport characteristics and the originally reported functional characterization of ZIP2 (1). Therefore, the goal of the current work was to reexamine and extend the functional characterization of ZIP2.

Material and Methods

Chemicals and Reagents - Unless mentioned, all the chemicals and reagents were purchased from Sigma-Aldrich

Cell culture methods - HEK293[2] cells were grown in complete Dulbecco's modified Eagle medium (Gibco) supplemented with 10% fetal bovine serum (FBS), 10 mM HEPES[3], 100 µM minimal essential medium non-essential amino acids and 1 mM sodium pyruvate (Gibco). Cells were cultured at 37 °C and 5 % CO_2 and subcultivated when confluency reached 90%.

Cells were transfected 24h after plating, following the manufacturer's protocol for the Lipofectamine 2000 (Invitrogen) reagent, using 50% of the recommended amount of human SLC39A2/ZIP2 (Uniprot ID: Q9NP94) encoding DNA and Lipofectamine 2000. The transfection medium was changed after 4 h. Transfection efficiency was estimated to be at least 70% using fluorescence microscopy.

Cd^{2+} flux measurements using the FLIPR Tetra - Cells were plated in 96-well, clear-bottom, black-well plates coated with poly-D-lysine at a density of 2 x 10^4 cells per well. The next day, cells were transfected with ZIP2-pIRES2 DsRed-Express2 or mock-transfected using lipotransfection. On the experimental day, the cell culture medium was replaced with 100 µl of loading buffer (modified Krebs buffer containing 117 mM NaCl, 4,8 mM KCl, 1 mM $MgCl_2$, 10 mM D-Glucose, 5 mM HEPES, 5 mM MES[4] and Calcium-5

[2] HEK293, Human embryonic kidney 293
[3] HEPES, 4-(2-hydroxyethyl)-1-piperazineethanesulfonic acid
[4] MES, 2-(N-Morpholino)ethanesulfonic acid

fluorescence dye (Molecular Devices), pH= 6.5). Cells were then incubated in the loading buffer at 37 °C for 1 h. Fluorescence Cd^{2+} measurements were carried out using a FLIPR-Tetra high throughput fluorescence microplate reader. Cells were excited using the 470–495 nm LED module, and the emitted fluorescence signal was filtered with a 515–575 nm emission filter. Cd^{2+} and the other tested solutes were prepared in assay buffer as 2x concentrated solutions in a separate 96-well plate. Establishment of a stable baseline was followed by addition of 100 µl of the indicated [Cd^{2+}] and measurements of fluorescence for 15 min. Measurements were made at 1-s intervals. In the negative control group, no substrate was administered. Results were exported from the FLIPR raw data as "Area Under the Curve" (AUC) of the fluorescence signal intensity in the interval after the addition of substrates (seconds 460-750). In sodium replacement experiments 120 mM NaCl were replaced by 120 mM choline chloride, NMDG[5] or KCl. In chloride replacements assays all the chloride containing salts were replaced by their corresponding equimolar gluconate salts. In pH-dependence experiments, the different pH were adjusted with 1N HCl/NaOH.

Oocyte Isolation and Injection - Capped cRNA was synthesized using a linearized cDNA template and the T7 mMessage mMachine kit (Ambion). *Xenopus laevis* oocytes were isolated and dissociated using collagenase as described (22) followed by injection with 50 nl of water or cRNA at 0.4 ng/nl (20 ng/oocyte), using a Nanoject-II injector (Drummond Scientific, Broomall, PA). Oocytes were maintained at 16°C in OR3 medium (22) and studied 3-6 days after injection.

Radioactive uptake - Zinc uptake into oocytes was measured by incubating groups of 8-10 *X. laevis* oocytes for 30 min in 1 ml of uptake buffer (ND96: 96 mM NaCl, 2 mM KCl, 1 mM $MgCl_2$, 1.8 mM $CaCl_2$, 5 mM MES, 1 mM HEPES, 1 mM Tris[6], pH 6.0) plus 100 µM $ZnCl_2$ including 0.05 µCi $^{63}Zn^{2+}$ (prepared as reported in ref.(23)).Oocytes were washed three times in uptake buffer plus 1 mM $ZnCl_2$ before measuring $^{63}Zn^{2+}$ incorporation into single oocytes as γ emission with a WIZARD2 gamma counter (Perkin Elmer). For $^{63}Zn^{2+}$ uptake at different pH the amounts of MES, HEPES and Tris were varied. To determine the effect of HCO_3^- on ZIP2 function 96 mM NaCl was replaced by 96 mM $NaHCO_3$ in the standard ND96. In sodium replacement assays 96 mM NaCl was replaced by 96 mM choline chloride or 96 mM KCl.

Radioactive iron uptake experiments in HEK293 cells were performed as described earlier (20). Briefly, cells were plated in 96-well, clear-bottom, white-well plates coated with poly-D-lysine at a density of 2 x 10^4 cells per well. The next day, cells were transfected with ZIP2-pIRES2 DsRed-Express2 or hDMT1-pIRES2 DsRed-Express2 using lipotransfection. On the experimental day, the growth medium was aspirated and cells were washed 3 times with Krebs–Ringer buffer (140 mM NaCl, 2.5 mM KCl, 1.2 mM

[5] NMDG, N-Methyl-D-glucamine
[6] Tris, 2-Amino-2-(hydroxymethyl) propane-1,3-diol

$MgCl_2$, 1.2 mM $CaCl_2$, 10 mM D-glucose, 5 mM HEPES, 5 mM MES pH = 7.4). To measure iron uptake the Krebs–Ringer buffer (pH = 5.5) was supplemented with 1 mM ascorbic acid, 1 μM $FeCl_2$ and 5 μCi/ml radioactive [^{55}Fe] iron. The assay was terminated after 15 min by washing the plates 4 times with ice cold Krebs–Ringer buffer. Subsequently, 100 μl of MicroScint-20 (PerkinElmer) were dispensed into each well and incubated at RT[7] for 1h under constant agitation. Radioactive [^{55}Fe] iron uptake was measured using a TopCount Microplate Scintillation and Luminescence Counter (PerkinElmer).

Two-electrode Voltage Clamp - Two-microelectrode voltage clamping (TEVC) was used to measure steady-state currents in control oocytes and oocytes injected with ZIP2 mRNA, 4–7 days after injection. Oocyte membrane currents were recorded using an OC-725C voltage clamp (Warner Instruments, Hamden, CT), filtered at 2–5 kHz, digitized at 10 kHz, and recorded with Pulse software, and data were analysed using the PulseFit program (HEKA), as previously described (22). Voltage microelectrodes (resistance 0.5–5 MΩ) were made from fiber-capillary borosilicate and filled with 3M KCl. Oocytes were perfused at room temperature in ND96 buffer. For periods when current-voltage (*I-V*) protocols were not being run, oocytes were clamped at a holding potential (V_h) of -60 mV. *I-V* protocols consisted of 100-ms steps-changes in membrane potential from -120 mV to +40 mV in 20-mV increments before and after the addition of the test substrate. The resulting data were filtered at 5 kHz (8 pole Bessel filter, Frequency Devices) and sampled at 1 kHz. *I-V* relationship was determined by plotting the mean steady-state current against voltage for a given set of experiments. Additionally, current was monitored continuously in oocytes clamped at V_h -60 mV. Test solutions were perfused at room temperature for several minutes until a steady-state current was observed.

pH Microelectrodes - Ion-selective microelectrodes were used to monitor intracellular pH (pH*i*) of ZIP2- and water-injected oocytes as previously described (22). Ion-selective electrodes were pulled similarly to those used for TEVC and silanized with bis-(dimethylamino)-dimethylsilane (Fluka Chemical Corp., Ronkonkoma, NY). Electrode tips were filled with hydrogen ionophore 1-cocktail B (Fluka) and back-filled with phosphate buffer at pH 7.0. Intracellular pH was measured as the difference between the pH electrode and a KCl voltage electrode impaled into the oocyte, and membrane potential (V_m) was the potential difference between the KCl and an extracellular calomel microelectrode. Electrodes were calibrated using pH 6.0 and 8.0 (Fisher), followed by point calibration in ND96 (pH 7.50). All pH microelectrodes used had slopes of at least -54 mV/ pH unit.

Confocal Cd^{2+}-flux imaging - *Single cell with clamped membrane potential; patch clamping* - Membrane potential was clamped to -60 mV using the patch clamp technique in the whole-cell configuration. The pipette solution was composed of:Cs-Asp[8] 120 mM, TEA-Cl[9] 20 mM, K_2ATP[10] 5 mM, NaCl 8 mM,

[7] RT, Room temperature
[8] Cs-Asp, Cesium-Aspartate

$MgCl_2$ 5.6 mM (free Mg^{2+} 0.75 mM) and HEPES 20 mM and 50 µM Fluo 3 pentapotassium salt. Note that, for this experimental set, in order to monitor Cd^{2+} fluxes, the Calcium 5 dye was replaced by Fluo-3, another calcium indicator that is sensitive to Cd^{2+} (24).The reason is because a membrane impermeable dye was required to avoid unspecific signal loss after cell loading. The pH was adjusted to 7.2 with CsOH and the osmolality was 285 mosmol/Kg. The external solution was composed of: NaCl 117 mM, KCl 4.8 mM, $MgCl_2$ 1 mM, D-Glucose 5 mM, HEPES 5 mM and MES 5 mM. The pH was adjusted to 6.5 with 1N HCl. In high potassium condition NaCl was replaced by equimolar KCl. All experiments were carried out at room temperature.

Confocal Cd^{2+} imaging - Multi-cells recording - Calcium-5 fluorescent dye (Molecular Devices) was used to record Cd^{2+} uptake. Prior to the measurements, cells were incubated 1h at 37ºC in the following external solution (in mM): NaCl 117, KCl 4.8, $MgCl_2$ 1, mM D-Glucose 10, HEPES 5, MES 5 and Calcium-5 dye). The pH was adjusted to 6.5 with HCl 1N. In high potassium condition NaCl was replaced by equimolar KCl. All experiments were carried out at room temperature.

Cd^{2+} images were acquired with a FluoView 1000 (Olympus) confocal laser-scanning microscope. Fluo-3 and Calcium-5 dye were excited at 473 nm with a solid-state laser and fluorescence was detected between 515 and 585 nm. To control cell transfection, DsRed-Express2 was excited at 561 nm or 488 nm with a solid-state laser and fluorescence was detected at >585 nm. Images were processed and analysed using the software ImageJ. The measurements are expressed as $\Delta F/F0$, whereby F0 is the fluorescence recorded before Cd^{2+} application.

Statistical analyses – The normal distribution of the experimental groups was determined by Kolmogorov-Smirnov (N>50) and Shapiro-Wilk (N<50) tests. Normally distributed independent experimental groups were compared by unpaired Student's test. When not normally distributed, Mann-Whitney U test was used to assess differences. Statistical test were performed using the IBM statistics 20 software. P values lower than 0.05 are considered statically significant.

Results

[9] Tetraethylammonium chloride
[10] Adenosine 5′-triphosphate dipotassium salt

Dependence of ZIP2 functional activity on extracellular pH - Based on the studies of Gaither et al., the functional activity of ZIP2 was found to be inhibited at pH levels below 7.0 (1). On the other hand, our fluorescence-based transport assay using transiently transfected HEK293 cells revealed that, at acidic pH (6.5), ZIP2-mediated Cd^{2+} transport was greatly increased compared to pH 7.5 (2). What could be the reason for this discrepancy? In our assay, pH changes may have influenced the binding affinity of the fluorescent-dye used (Calcium 5) to measure Cd^{2+}. Also, Cd^{2} rather than Zn^{2+} transport was measured which might account for the reversed pH dependence. We therefore decided to perform additional experiments to evaluate this incongruity. To this end, we used the standard radioactive tracer method using *Xenopus laevis* oocytes as an expression system, thus ensuring the same functional readout as used by Gaither et al in their studies. Using this methodology, the effect of variable extracellular pH values (pH 5.0 - 8.2) on ZIP2-mediated $^{63}Zn^{2+}$ uptake was determined (Figure 1A). Whereas the water-injected oocytes showed only a slight pH-dependence of endogenous Zn^{2+} transport activity, ZIP2 transport activity was maximal at acidic pH <6.0 and almost negligible at pH >7.5. These results confirmed our previous findings (2) and further validate our fluorescence assay which was used as a screening assay to identify ZIP2 modulators.

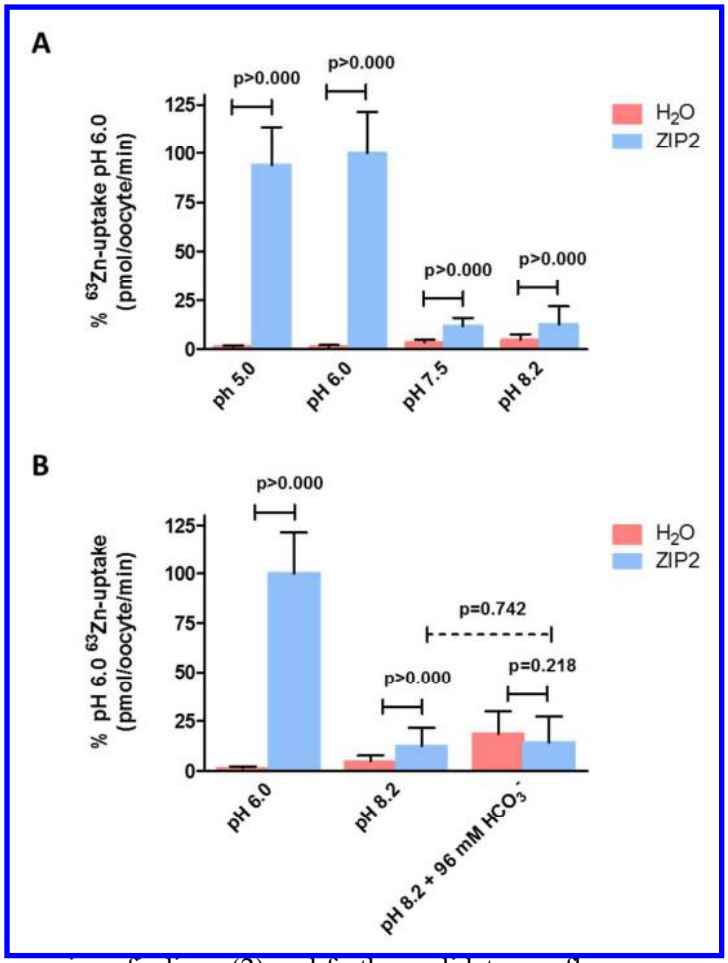

Fig. 1. Effect of extracellular pH and bicarbonate upon $^{63}Zn^{2+}$ uptake by ZIP2-expressing X. laevis oocytes. Uptake of $^{63}Zn^{2+}$ in the presence of 100 µM $ZnCl_2$ by ZIP2- and H_2O-injected X. laevis oocytes was measured at (**A**) different extracellular pH (pH 5-8.2) and (**B**) in the absence (pH 6 and 8.2) and presence of HCO_3^- (96 mM) at pH 8.2. Data from 3 different batches of oocytes were normalized to the mean Zn^{2+} uptake by ZIP2 at pH 6.0 (580 ± 124 to 403 ± 62 pmol/oocyte/min) and are represented as the Mean ± S.D. (6 to 26 oocytes).

Zn^{2+} transport mediated by ZIP2 is not coupled to HCO_3^- - It was previously proposed that ZIP2 operates as a Zn^{2+}/HCO_3^- cotransporter (1). We aimed to confirm this hypothesis by measuring $^{63}Zn^{2+}$ uptake by ZIP2 cRNA[11] microinjected *X. laevis* oocytes in the presence and absence of HCO_3^-. To this end, we replaced the [NaCl] of the uptake solution by equimolar [$NaHCO_3$] which resulted in a pH of 8.2. Since adjusting the pH of the solution would alter [HCO_3^-], we compared the $^{63}Zn^{2+}$ uptake in the HCO_3^--containing solution with the normal uptake solution, both at pH 8.2 (Figure 1B). We did not observe a difference in the transport activity of ZIP2, whereas the H_2O-injected oocytes showed a higher activity at increased [HCO_3^-]. Additionally, in order to confirm these findings, we used pH sensitive microelectrodes

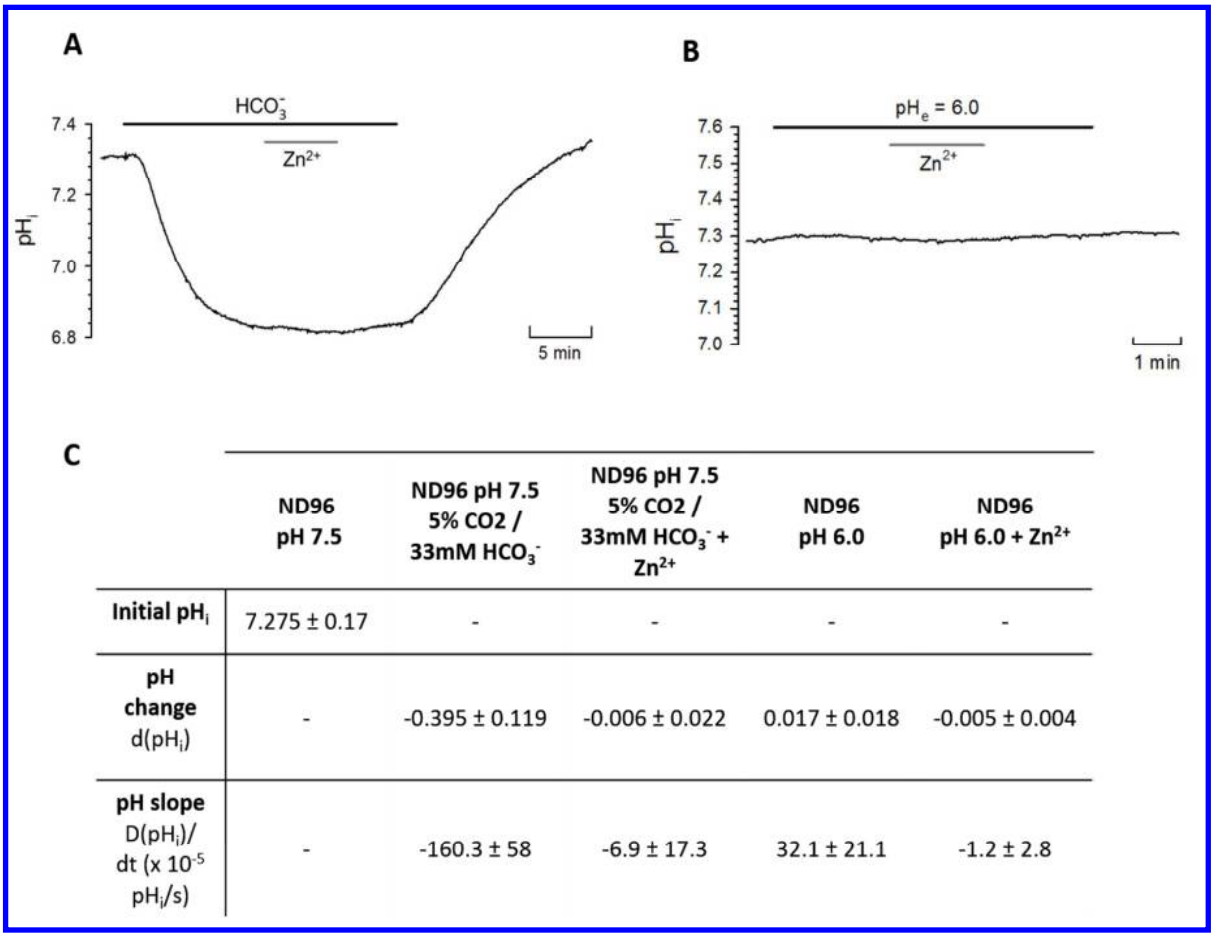

C

	ND96 pH 7.5	ND96 pH 7.5 5% CO2 / 33mM HCO_3^-	ND96 pH 7.5 5% CO2 / 33mM HCO_3^- + Zn^{2+}	ND96 pH 6.0	ND96 pH 6.0 + Zn^{2+}
Initial pH_i	7.275 ± 0.17	-	-	-	-
pH change $d(pH_i)$	-	-0.395 ± 0.119	-0.006 ± 0.022	0.017 ± 0.018	-0.005 ± 0.004
pH slope $D(pH_i)/dt$ (x 10^{-5} pH_i/s)	-	-160.3 ± 58	-6.9 ± 17.3	32.1 ± 21.1	-1.2 ± 2.8

Fig. 2 Role of bicarbonate and protons on zinc uptake by ZIP2-expressing *X.laevis* oocytes. Representative trace of intracellular pH (pH_i) changes in response to perfusion of CO_2 (5%)/HCO_3^- (33 mM) (**A**) or ND96 pH 6.0 (**B**) in the absence and presence of Zn^{2+} (100 µM). Transport activity of ZIP2 was monitored as change in pH_i when Zn^{2+} was added and removed extracellularly. **C**) Summary table of the pH change and pH slope (10^{-5} pH units/s) determined after the perfusion of each of the different media. Results are the Mean ± S.D. (2-6 oocytes).

[11] cRNA, complementary RNA

to measure intracellular pH (pH_i[12]) changes due to HCO_3^--coupled Zn^{2+} transport via ZIP2 expressed *X. laevis* oocytes (Figure 2A). The uptake buffer was equilibrated by addition of 5% CO_2 / 33 mM HCO_3^-. The CO_2 caused an acidification in ZIP2-injected oocytes (Figure 2A and C) as well as in H_2O-injected oocytes (data not shown). Upon perfusion of Zn^{2+}, the pH_i did not change, contradictory to what would be expected if the transport was coupled to HCO_3^- (Figure 2A and C).

ZIP2 does not transport H^+ - Our experiments suggests that H^+ may be involved in the ZIP2-mediated transport process. Thus, we also used the pH sensitive microelectrodes in *X. laevis* oocytes to investigate whether protons are coupled to ZIP2 mediated Zn^{2+} transport (Figure 2B). Almost no change was observed when the pH 7.5 uptake solution was replaced by pH 6 solution, indicating that there is no H^+ permeation via ZIP2. Also, addition of Zn^{2+} did not cause a significant change in pH_i in ZIP2-injected oocytes (Figure 2B and C). These results indicate that ZIP2 does not facilitate transport of H^+, neither alone nor coupled to Zn^{2+} transport.

ZIP2 is not electrogenic - To test whether ZIP2-mediated Zn^{2+} transport is electrogenic, functional experiments were performed using two-electrode-voltage-clamp (TEVC[13]). We did not observe any discernible change in the current-voltage (*I-V*[14]) relationship following step-changes in membrane potential (V_m[15]) of oocytes expressing ZIP2 at extracellular pH 7.5 or 6.0 (Figures 3A and B). Moreover perfusion of Zn^{2+} (100 μM) did not evoke any appreciable change in the *I-V* relationship (Figures 3A and B). Similar results were obtained when current was monitored continuously in oocytes clamped (V_h[16]) at -60 mV (data not shown). Hence, functional experiments performed with TEVC indicate that there are no measurable currents associated with ZIP2-mediated Zn^{2+} transport which is surprising, given the positive charge of the divalent metal ion Zn^{2+} and the highly significant transport activity observed for ZIP2 cRNA-injected oocytes when measuring $^{63}Zn^{2+}$ accumulation under similar experimental conditions (Figure 1).

[12] pH_i, intracellular pH
[13] TEVC, two-electrode-voltage-clamp
[14] I-V, Intensity-voltage
[15] V_m, membrane potential
[16] V_h, holding voltage

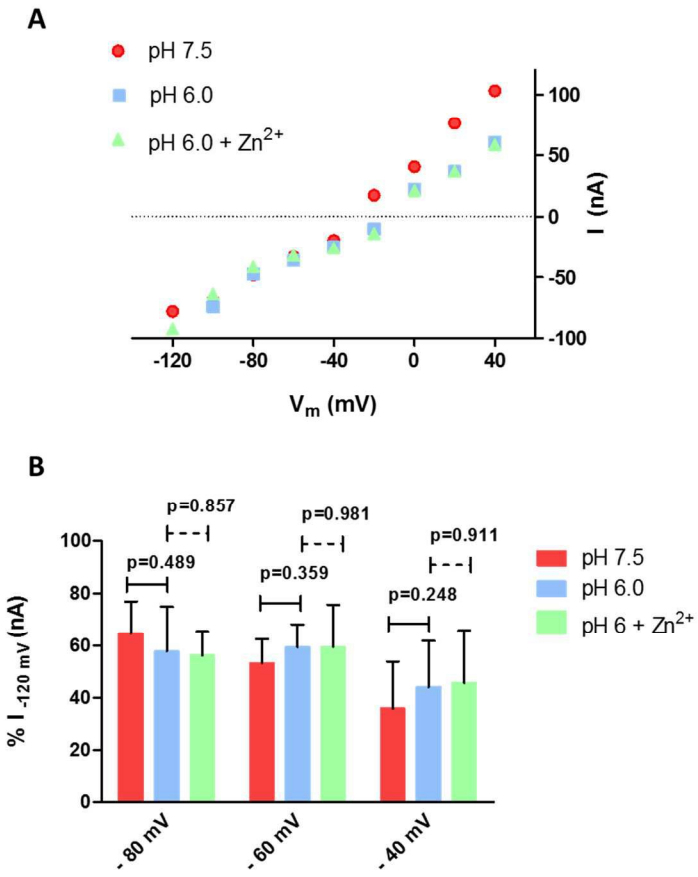

Fig. 3. Electrophysiological properties of ZIP2-expressing X.laevis oocytes. A) Representative trace of the current-voltage relationship under the indicated conditions (V_h = -60 mV; 100 µM Zn^{2+}). **B)** Average currents recorded under the indicated conditions. For each individual oocyte the data were normalized to the current recorded at -120 mV in pH 7.5 medium (-159.37 to -38.75 nA). Data from the different oocytes (n = 6) were pooled together and are represented as the Mean ± S.D.

Transport mediated by ZIP2 is not dependent on Na^+ or Cl^- gradients, but is inhibited by K^+ - We investigated whether ZIP2-mediated transport is coupled to Na^+, K^+ or Cl^-, by isosmotic replacement of these ions in the standard uptake solution. To address this question, we used both a fluorescent-based Cd^{2+} influx assay (Fig. 4A) in transiently transfected HEK293 cells and a $^{63}Zn^{2+}$ uptake assay in ZIP2-cRNA-injected *X. laevis* oocytes (Fig. 4B). [Na^+] was replaced by equimolar [NMDG], [choline] or [K^+], whereas [Cl^-] was replaced by the corresponding gluconate salts. Replacement of Na^+ with NMDG or

choline had no effect on ZIP2 activity, whereas replacing it by K^+ reduced transport by ≈ 60-40 %. Replacement of chloride by gluconate salts did not have any effect on ZIP2 activity.

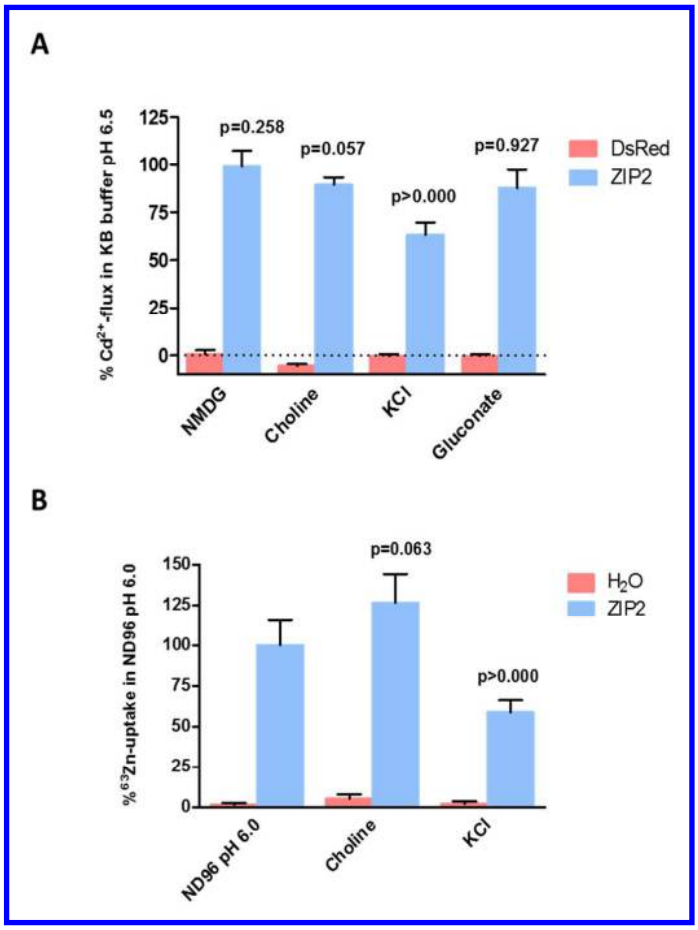

Fig. 4. Effect of sodium, chloride and potassium extracellular concentration over ZIP2 transport activity. A) Changes of fluorescence intensity of Calcium-5-dye in response to Cd^{2+} perfusion (1 µM) measured in HEK293 cells transiently transfected with DsRed Express2 and ZIP2 DNA constructs in KB buffer pH 6.5 in which extracellular [Na+] or [Cl-] were replaced by equimolar [NMDG], [Choline+] and [K+] or [Gluconate salts] respectively. Data from 2 independent experiments were normalized to the mean ZIP2 activity at pH 6.5 and are represented as the Mean ± S.D. (n = 8-12). **B**) Uptake of $^{63}Zn^{2+}$ in the presence of 100 µM ZnCl2 by ZIP2- and H2O-injected X. laevis oocytes was measured in ND96 pH 6.0 in which extracellular [Na+] was replaced by equimolar [Choline+] or [K+]. Data from 2 different batches of oocytes were normalized to the mean Zn^{2+} uptake by ZIP2 at pH 6.0 (403 ± 62 pmol/oocyte/min) and are represented as

Transport mediated by ZIP2 is not coupled to K^+, but it is voltage-dependent - To clarify whether the reduction in ZIP2-mediated Cd^{2+} or Zn^{2+} transport when replacing Na^+ by K^+ is due to direct K^+-coupled metal ion transport or merely a result of membrane depolarization generated by increased extracellular [K^+], fluorometric analysis under voltage-clamp condition was conducted. First, fluorometric measurements were carried out without voltage clamping, within an open field of ZIP2 transfected cells (Fig. 5A, B and C). In line with our previous observations, [Na^+] replacement by equimolar [K^+] induced an inhibition ≈ 40% of the ZIP2-mediated influx of Cd^{2+}. Next, the same procedure was performed in individual cells under voltage-clamp conditions (V_h= -60 mV) (Fig. 5D, E and F). Interestingly, under

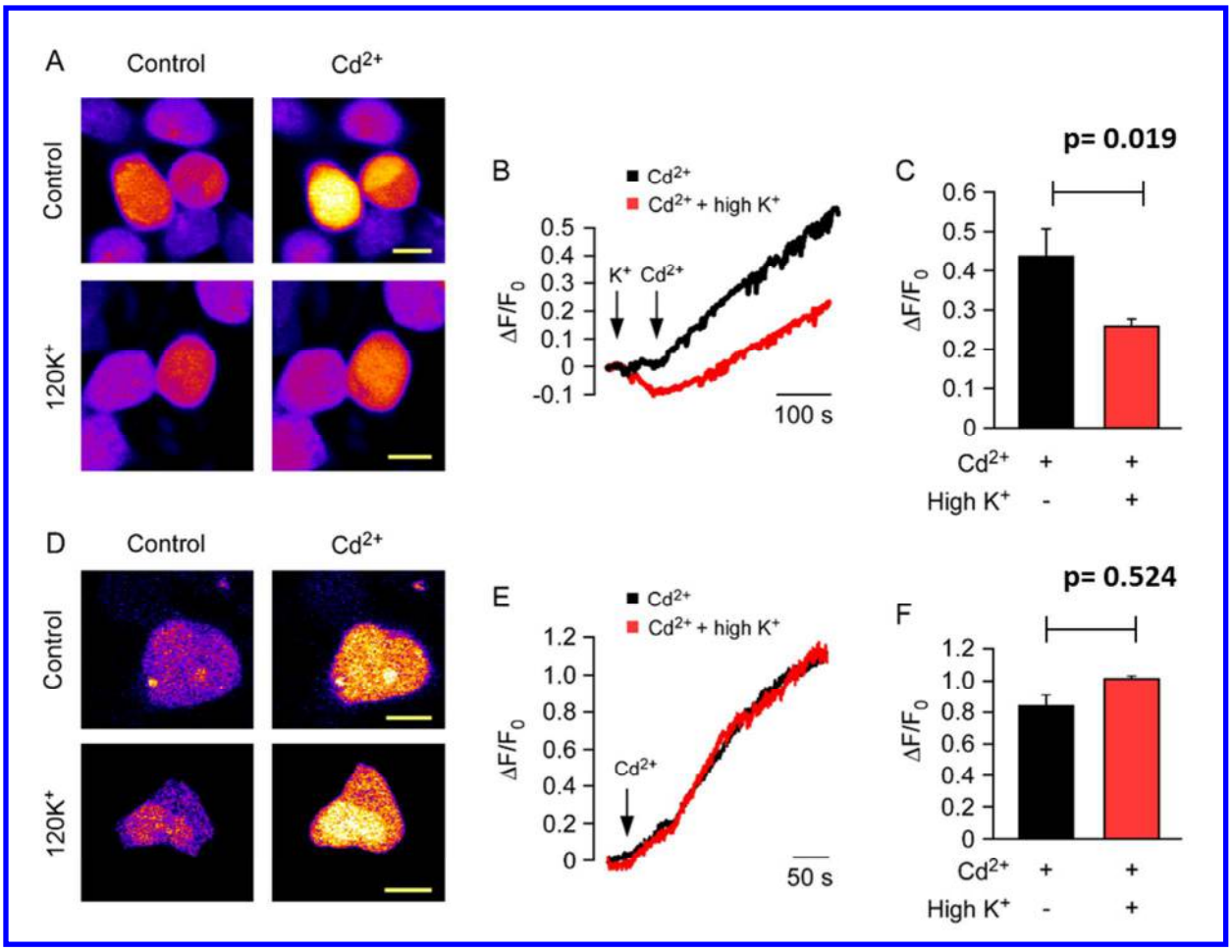

Fig.5. Effect of potassium over membrane potential in ZIP2 transiently transfected HEK293 cells. Representative images of intact (**A)** or dialyzed (**D**) cells before and after the treatment with Cd^{2+} (10 µM) in the presence (control) or absence of extracellular 120 mM K^+. Representative traces of Cd^{2+}-flux induced changes on fluorescence intensity in intact (**B**) and clamped (**E**) cells in the presence and absence of 120 mM K^+. Fluorescence intensity changes were measured as $\Delta F/F_0$ (where F_0 is the signal before Cd^{2+} application). Data from 3 and 5 independent experiments for intact (n=38-41) and dialyzed (n= 8-10) cells, respectively, were represented as Mean ± S.D.

voltage-clamp conditions, the inhibition was lost and the ZIP2-mediated influx of Cd^{2+} was similar in the presence and absence of high extracellular [K^+]. These results demonstrate that K^+ is not part of the translocation mechanism of ZIP2 and that transport is voltage-dependent.

Transport kinetics and pH-dependence of ZIP2 - The kinetics of ZIP2-mediated transport was studied using our Cd^{2+}-flux fluorescence-based assay in transiently transfected HEK293 cells. Fluorescence

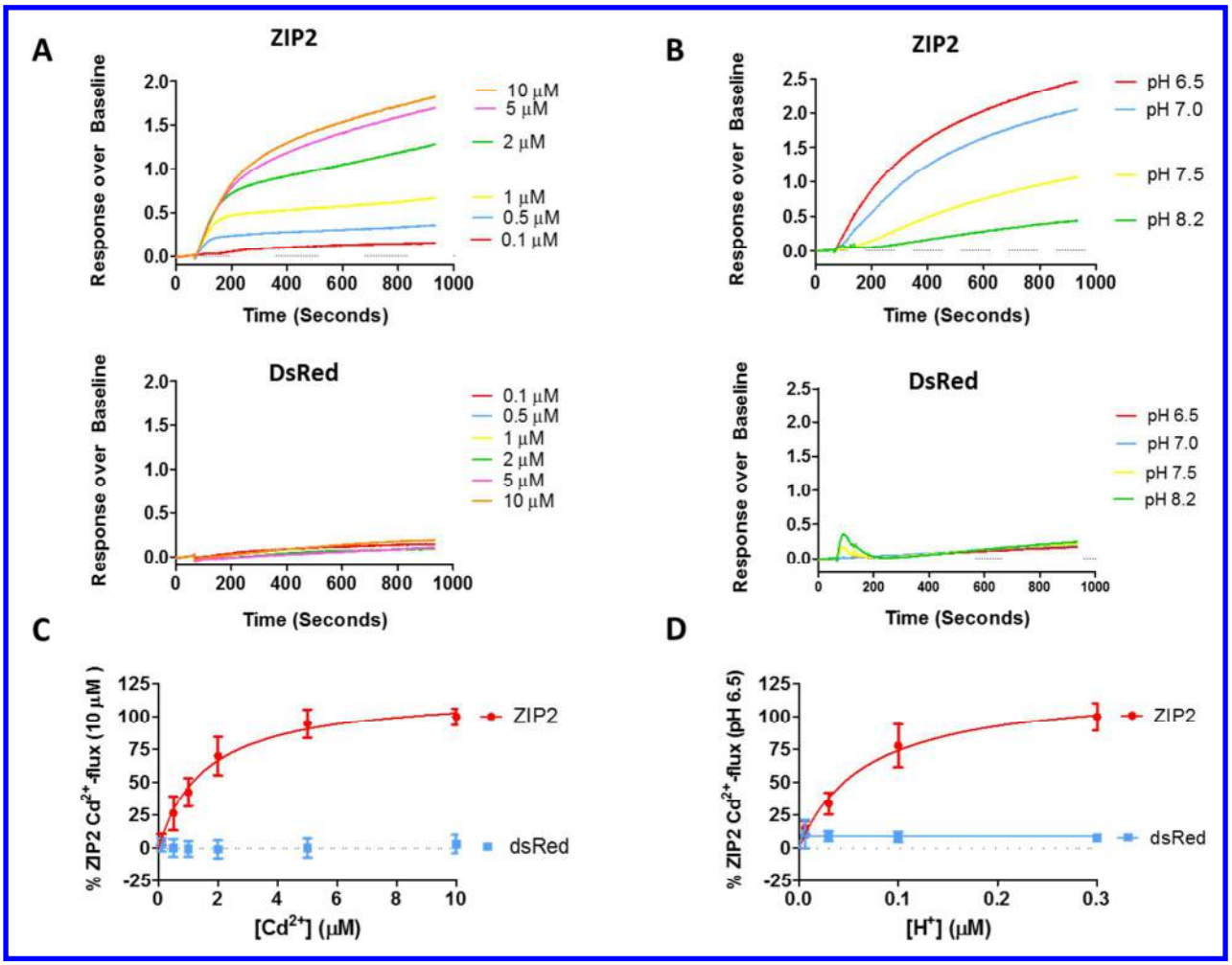

Fig. 6. Kinetics and pH-dependence of the Cd^{2+} transport measured in ZIP2 or DsRed Express2 (empty vector) transiently transfected HEK293 cells. Representative experiments showing the changes on fluorescence intensity of Calcium-5-dye in response to the perfusion of different Cd^{2+} concentrations (0.1-10 µM) at extracellular pH 6.5 (**A**) or at different extracellular pH values (6.5-8,2) in the presence of saturating concentration of Cd^{2+} (10 µM) (**B**). To determine the Kinetics (**C**) and pH-dependence (**D**) of Cd^{2+} transport, the Area under the curve (AUC) for each single trace was calculated. Data from 3 independent experiments were normalized to the mean Cd^{2+} uptake by ZIP2 at pH 6.5 (337.22 ± 34 to 890 ± 22 AUC), collected and are represented as the mean ± S. D. (n = 7-28). Kinetic parameters were obtained by fitting the data points to the Michaelis-Menten equation (solid lines).

intensity changes increased with extracellular [Cd^{2+}] (Fig.6A; upper panel). Measuring Cd^{2+}-flux through ZIP2 gave a dose-response curve that saturated at 5 μM [Cd^{2+}] (Fig. 6C). The calculated apparent affinity constant K_m for Cd^{2+} was ~ 1.57 ± 018 μM. Empty-vector transfected cells did not show any change in fluorescent intensity within the range of [Cd^{2+}] tested (Fig.6A; lower panel).

Using the same methodology, the pH-dependence of the ZIP2-mediated transport was studied. In line with our previous findings, fluorescent intensity changes after Cd^{2+} (10μM) perfusion increased with the extracellular [H^+] (Fig.6B; upper panel). Transport was completely saturated at extracellular pH 6.5 and the calculated apparent affinity was K_{H+} ~ 66 ± 16 nM, corresponding to pH ~7.2 (Fig.6C). Again, no effect was observed over the empty-vector transfected cells (Fig.6B; lower panel).

Cation selectivity of ZIP2 - In order to investigate the cationic selectivity of ZIP2, Cd^{2+}-flux was measured in the presence of high extracellular concentrations (50 μM) of different divalent cations such as Ba^{2+}, Mn^{2+}, Co^{2+}, Zn^{2+} and Cu^{2+} (Fig. 7A). Note that none of these metal ions showed significant interactions with the Calcium 5 dye when high concentrations of them (100 μM) were perfused individually into ZIP2 overexpressing cells (data not shown). As expected, in the presence of Zn^{2+}, Cd^{2+}-flux was completely inhibited. Interestingly, Cu^{2+} and Co^{2+} inhibited 75% and 25%, respectively, of the Cd^{2+}-flux, while no significant inhibition was observed by Ba^{2+} or Mn^{2+}. Fe^{2+} is another putative substrate of ZIP2. However, since it also interacts with the Ca^{2+}-5-dye, it was not included in this set of experiments. To overcome this issue, we measured directly the radiolabeled iron ($^{55}Fe^{2+}$) uptake (Fig. 7B). As a positive control for this assay, we used the human divalent metal transporter 1 (hDMT1, SLC11A2) (25). $^{55}Fe^{2+}$-uptake by ZIP2 was not significantly different from that of empty vector-transfected cells and 7-fold lower than the uptake mediated by hDMT1, demonstrating that Fe^{2+} is not substrate of ZIP2.

To determine the apparent affinity of ZIP2 for Zn^{2+} and Cu^{2+}, Cd^{2+}-flux was measured in the presence of a range of extracellular concentrations of Zn^{2+} or Cu^{2+}. In both cases, inhibition of Cd^{2+}-flux gave dose-response sigmoidal curves. The calculated IC_{50} values were ~ 0.52 ± 1.7 μM for Zn^{2+} (Fig. 7C) and ~ 2.98 ± 1.3 μM for Cu^{2+} (Fig. 7D). Given that the K_m of ZIP2 for Cd^{2+} is 1.57 μM (Fig. 6C), according to the Cheng-Prusoff equation (26), the IC_{50} values for Zn^{2+} and Cu^{2+} are 0.32 μM and 1.81 μM respectively. Hence, the cationic selectivity for ZIP2 decreases in the order $Zn^{2+} > Cd^{2+} \geq Cu^{2+} > Co^{2+}$, while Fe^{2+}, Mn^{2+} and Ba^{2+} are not transport substrates.

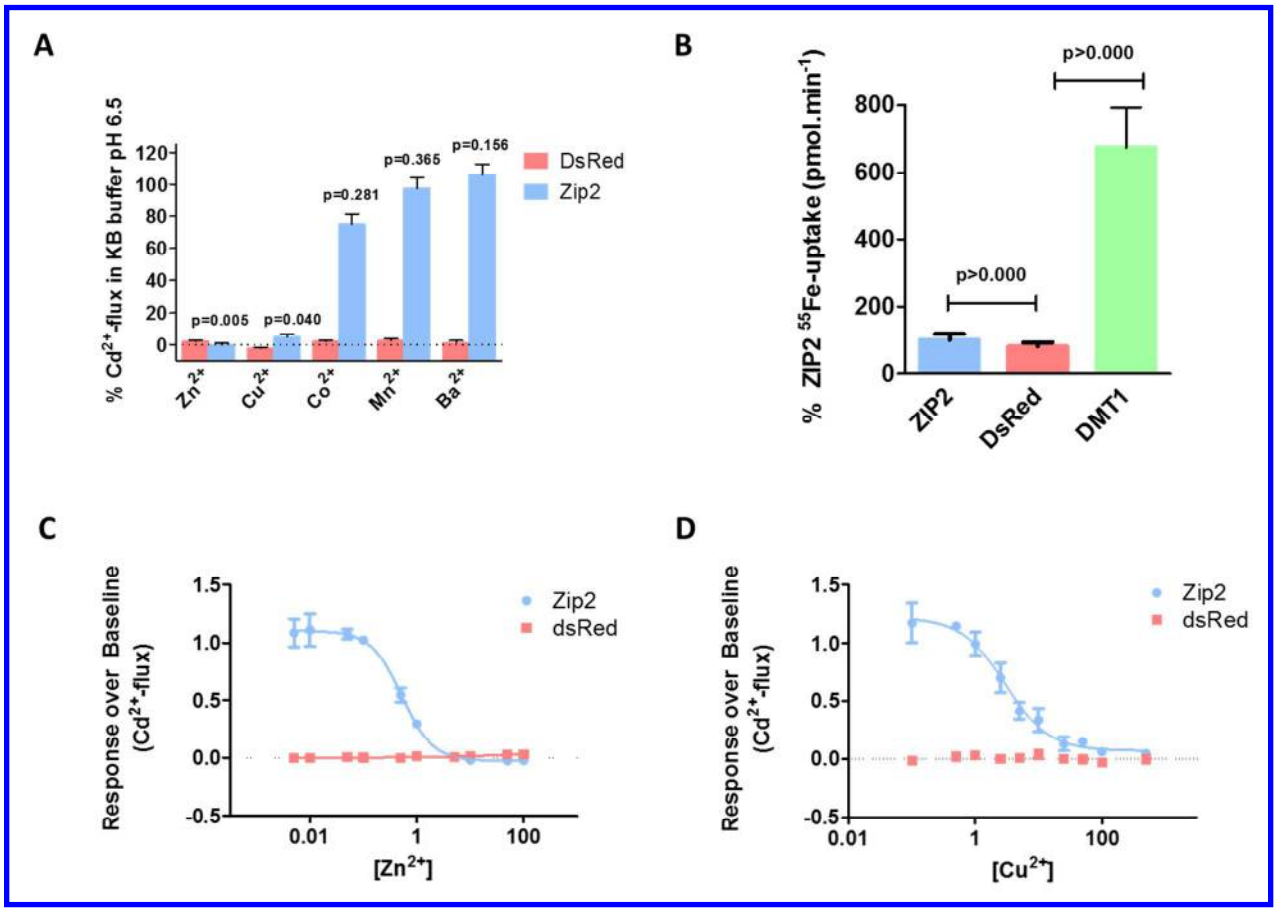

Fig. 7. Divalent cation selectivity of ZIP2 in transiently transfected HEK293 cells. A) Changes of fluorescence intensity of Calcium-5-dye in response to Cd^{2+} perfusion (1 µM) measured in the presence of the indicated divalent cations (50 µM) at pH 6.5. Data from 2 independent experiments were normalized to the mean ZIP2 activity at pH 6.5 in the absence of divalent cations other than Cd^{2+} (1µM) and are represented as the mean ± S.D. (n = 5-8). P-values establish statistical differences between ZIP2 mediated Cd^{2+}-uptake in the absence *Vs* the presence of the indicated divalent metals **B)** Uptake of $^{55}Fe^{2+}$ in the presence of 1 µM $FeCl_2$ and 100 µM Ascorbic Acid by HK293 cells transiently transfected with ZIP2, DsRed Express2 (empty vector) and DMT1 DNA constructs at extracellular pH 5.5. Data from 2 independent experiment were normalized to the mean ZIP2 $^{55}Fe^{2+}$ transport (0.09 ± 0.01 to 0.15 ± 0.02 $pmol.min^{-1}$) and represented as the mean ± S.D. (n =19-48). Inhibition of the ZIP2-mediated Cd^{2+} transport (1 µM) by increasing extracellular [Zn^{2+}] (**C**) and [Cu^{2+}] (**D**). Data from 2 independent experiments were normalized to the mean ZIP2 activity at pH 6.5 in the absence of divalent cations other than Cd^{2+} and are represented as the mean ± S.D. (n = 7). Inhibitory kinetics were obtained by fitting the data points to a 4-parameter sigmoidal equation (solid lines).

Discussion

In our functional experiments using different approaches, ZIP2-mediated transport was increased at acidic pH, even though no cotransport with H^+ was observed. We therefore conclude that the ZIP2 transport process is modulated by extracellular pH, independent of the H^+ driving force. Transport was not stimulated by the presence of HCO_3^-, as previously reported (1). Thus, we conclude that ZIP2-mediated transport is not coupled to bicarbonate. Also, in contrast to the previous observations (1), our experiments revealed that increasing extracellular [K^+] inhibits ZIP2-mediated metal ion uptake under non-voltage clamp condition. However, when the K^+ inhibitory effect was measured under voltage-clamp condition, it was abolished. This indicates that the inhibitory effect was due do the depolarization caused by increasing extracellular K^+ concentration to 140 mM. Therefore, we concluded that ZIP2-mediated metal ion transport is voltage dependent and, given the positive charge of Zn^{2+}, we expected that transport would be electrogenic.

Paradoxically, our electrophysiological analysis revealed that ZIP2-mediated Zn^{2+} transport is electroneutral. The electrophysiological experiments were done with ZIP2 overexpressed in *X. laevis* oocytes and in the presence of a robust inwardly directed electrochemical Zn^{2+} gradient, favouring transmembrane influx (i.e. membrane voltage was kept constant at -60mV and 100 μM $ZnCl_2$ was perfused). Using the same experimental approach, our group observed prominent transmembrane inward currents for Fe^{2+} transport via DMT1 expressed in *X. laevis* oocytes, even at neutral pH (that is in the absence of an inwardly directed H^+-gradient) (27). Given that ZIP2 injected oocytes exhibited high ^{63}Zn accumulation as shown in Figure 1, this rules out any issue related to plasma membrane expression. To explain the lack of electrogenicity, we propose the following:

1. Transport is still electrogenic but the turn-over rate of the transport process is too slow to allow any detection of transport-associated currents.
2. Transport is electroneutral because there are is and as yet unidentified coupling ion (via cotransport of exchange) that balances the positive charges of Zn^{2+}. In this case, given the voltage dependence of the transport process, the transport cycle must contain steps that are limited by the membrane potential.

Interestingly, the transport features of ZIP2 resemble those of a ZIP transporter from the Gram-negative, rod-shaped bacterium *Bordetella bronchiseptica* (ZIPB[17]) (28). In that work, ZIPB was described as a selective electrodiffusional channel, in which Zn^{2+} uptake is driven only down its concentration gradient. Remarkably, Zn^{2+} transport by ZIPB was modulated by the effect of K^+ on the resting membrane potential, indicating that ZIPB is also voltage-dependent. Furthermore, ZIPB-mediated Zn^{2+}-flux was modulated by pH and not stimulated by HCO_3^-. Also in line with our findings, *Fugu* pufferfish ZIP2, sharing 30% and 60% sequence identity with human ZIP2 and ZIP3, respectively, exhibited, when

[17] ZIPB, *Bordetella bronchiseptica* ZrT/Irt-like protein

expressed in MDCK[18] cells, Zn^{2+}-mediated transport in a pH-dependent manner. Transport was stimulated by acidic pH medium (pH 5.5-6.5) but was not enhanced (but rather slightly inhibited) by the presence of extracellular HCO_3^- (29).

Altogether, given that ZIP2-mediated transport is ATP-independent (1) and not coupled to Na^+, H^+, K^+, HCO_3^- or Cl-, we propose that Zn^{2+} uptake occurs via simple passive transport. Given that Zn^{2+} is a trace element essential for most mammalian cells, efficient uptake mechanisms must exist to allow cells to accumulate Zn^{2+}. Because intracellular Zn^{2+} is complexed with specific binding proteins, cytoplasmic Zn^{2+} concentrations are kept at very low (femtomolar to picomolar) levels. Consequently, the inwardly directed electrochemical Zn^{2+} gradient is expected to be sufficient to facilitate cellular Zn^{2+} uptake, supporting this concept of passive ZIP2-mediated transport (28).

The only ion showing interaction with the transport process mediated by ZIP2 is H^+. Our results show that, at low extracellular pH, transport of Zn^{2+} is increased. However, H^+ was not cotransported with Zn^{2+} and there was transport at pH >7.5, indicating that ZIP2-mediated transport is modulated by pH, rather than H^+ acting as a coupling ion. In addition to the aforementioned ZIPB and *Fugu* pufferfish ZIP2, there are many examples of ion channels that can be modulated by external pH, including Cl^- channels (30), Na^+ channels (31) and aquaporins (32), among others (33). In these channels, the protonation state of specific titratable residues affects voltage-dependence or gate-opening, leading to modulation of channel permeation. Future structure-function studies of ZIP2 to identify amino acidic residues responsible for H^+-sensitivity will shed further light on this pH modulatory mechanism.

As described previously, ZIP2 expression has been found in prostate epithelial cells (34), peripheral blood mononuclear cells of patients with tuberculosis and asthma (5) and epidermal keratinocytes (4). Interestingly, these tissues/cell types are involved in physiological processes occurring under an acidic environment. The main function of the prostate is to secrete prostatic fluid, which is acidic (6.5-6.7) (34,35). Based on its apical membrane localization, ZIP2 is hypothesized to help maintain prostate Zn^{2+} homeostasis by reabsorbing Zn^{2+} from the prostatic fluid. (3). Similarly, acidification of the airways linked to different pathological processes, including inflammation, ischaemia or aspiration of refluxing gastric contents, and obstructive airway diseases such as asthma, may lead to increased ZIP2-mediated transport (33). ZIP2 expression has been described in the epidermis and, moreover, transporter-mediated Zn^{2+} uptake is necessary for the differentiation of keratinocytes (4). The surface of healthy skin has a pH oscillating between 4.0 and 6.0 (36). Altogether, these findings further support the role of H^+ on the transport processes mediated by ZIP2 since, as our functional experiments point out, the functional activity of ZIP2 will be increased in these acidic environments. In turn, it seems counterintuitive to use HCO_3^- as driving force for the transport of Zn^{2+} under such physiological conditions as, at reduced pH, a

[18] MDCK, Madin-Darby Canine Kidney cells

significant part of bicarbonate will be in the conjugated acid form carbonic acid (H_2CO_3) (pKa = 6.2 at 37°C). In this regard, upregulation of ZIP2 expression in peripheral blood mononuclear cells of patients with tuberculosis was accompanied by down-regulation of the expression of SLC39A8 (ZIP8), and the authors proposed that this could be a consequence of changes in the pH and Zn^{2+} concentrations (5). These findings suggest a complementary function of ZIP2 and ZIP8. In line with this, our preliminary experiments using the herein described fluorescent based-assay, revealed opposite pH modulation for ZIP8 compared to ZIP2 (data not shown).

With respect to the kinetic properties of ZIP2, our experiments indicate that the K_m for ZIP2-mediated Cd^{2+} flux was ~ 1.6 μM, similar to that reported by Gaither and Eide for Zn^{2+} (K_m~ 3 μM) (1). On the other hand, based on our assay, ZIP2-mediated transport reached V_{max} already at 5 μM Cd^{2+} whereas in the study of Gaither *et. al*., V_{max} for Zn^{2+} transport was 20-40 μM (1). Another difference between the two studies exists when comparing the divalent metal competition experiments. According to our experiments, ZIP2 can transport Zn^{2+} and Cd^{2+} but not Fe^{2+}, and Cu^{2+} and Co^{2+} are likely also substrates, while $Ba^{2+}$and Mn^{2+} were not transported by ZIP2. In contrast, Gaither et al. proposed that all of these metals ions could serve as substrates of ZIP2 (1). In line with our findings, studies with HEK293 cells overexpressing mouse ZIP2, showed similar Michaelis-Menten kinetics for Zn^{2+} (K_m~ 1.6 μM) (37). Moreover, Zn^{2+} transport was inhibited in this study by excess of Cu^{2+}, Cd^{2+}, Co^{2+}, but not Fe^{2+} or Mn^{2+}. In contrast, the previously mentioned pufferfish ZIP2 exhibited ten-fold lower affinity for Zn^{2+} (K_m~ 13 μM), while Zn^{2+} transport was inhibited by Cu^{2+}, Cd^{2+}, Co^{2+}, Fe^{3+} and to lower extend by Fe^{2+} (29). This variabilities among competition experiments highlights the importance of determining the substrate selectivity of transporters by direct measurements of each putative substrate. In this regard, direct measurements of ^{63}Zn (Figure 1 and 4B), Cd^{2+} (Figure 6) and ^{55}Fe uptake (Figure 7B) confirm that Zn^{2+} and Cd^{2+} are real substrates of ZIP2, while iron was not found to be a substrate. Regarding to the other proposed ZIP2 substrates (i.e. $Cu^{2+}$and Co^{2+}), direct measurements will be required as well to verify them as transport substrates.

The incongruities between the current work and that of Gaither *et. al*. are likely due to the use of different expression systems. Gaither *et. al*. used the chronic myeloid leukaemia cell line K562 for their radiolabelled Zn^{2+}-uptake experiments. These cells endogenously express Zn^{2+} transporters, as well as the sodium-proton exchanger NHE1 (SLC9A1) (38) and the chloride/bicarbonate anion exchanger AE2 (SLC4A2) (39). Thus, the reported Zn^{2+} transport activities and divalent metal ion specificities in K652 cells represent the sum of both endogenous and expressed ZIP2 transporters. In addition, the inverse pH-sensitivity and role of bicarbonate in ZIP2-mediated transport could be related to interfering activities of NHE1 and AE2. Our functional experiments were conducted in HEK293 cells, which express endogenous NHE3 (SLC9A1) (40) but not AE2 (41). Also, experiments were done in *Xenopus* oocytes, which express

an NHE exchanger homolog but not any endogenous anionic exchangers (42). As functional readouts, we used a combination of different methods, including electrophysiological measurements, radiolabelled Zn^{2+}-uptake experiments in *X.laevis* oocytes and Cd^{2+}-flux based fluorescent assay in HEK293 cells. Importantly, in non-injected control oocytes or in empty-vector transfected HEK cells, endogenous Zn^{2+}-transport (Figure 1) or Cd^{2+}-transport (Figure 6A) was negligible compared to ZIP2 expressing oocytes or cells. Hence, our experimental approaches guarantee an optimal signal-to-noise ratio for studying different aspects of the ZIP2 transport mechanism. This allowed us to validate our observations using different techniques, thereby generating data with great consistency, as demonstrated, for example, for the pH-dependence (Figures 1A and 6B) or the effect of K^+ (Figures 4 and 5).

We anticipate that the herein reported data are valuable to predict the putative roles of ZIP2 in pathological situations or during physiological challenges. Indeed, human genetic studies revealed that ZIP2 polymorphisms constitute a risk factor for a wide variety of human diseases, including carotid artery disease in aging (43), arsenic-related bladder cancer (44) and cystic fibrosis (45). In addition, ZIP2 activity is important for prostate function and related to prostate cancer development (3,34), keratinocyte differentiation (4) and macrophage (46) and monocyte function (13). Also ZIP2 knockout mice studies revealed increased susceptibility to Zn-deficiency during pregnancy (19). As a follow-up, specific experiments are needed to unveil the particular roles of ZIP2 in physiologically relevant environments. For example, functional studies with the aforementioned genetic variants will be required to reveal the precise molecular mechanisms leading to the associated disease conditions. Also, tissue specific knockout studies in cellular or animal models are required to describe the physiological and pathological impacts of ZIP2 dysfunction. Such studies may in turn accelerate the discovery of therapeutic applications targeting ZIP2.

Conclusion

Our data show that ZIP2-mediated transport is modulated by extracellular pH, in an H^+ driving-force independent and voltage-dependent manner. Accordingly, we propose that ZIP2 is a facilitative transporter that mediates transport of Zn^{2+} down its concentration gradient, which can be modulated by interaction of H^+ with titratable acidic amino acid residues within the ZIP2 protein. Specifically, we propose that protonation of such a titratable amino acid stabilizes the ZIP2 protein in a conformation in which substrate transport is more favourable. This would explain why the transport rate is increased in the presence of H^+. ZIP2 is expressed in acidic environments, where this regulatory mechanism is expected to be important to speed up and determine the direction of the transport process.

The herein proposed transport mechanism is consistent with those of ZIPs from lower organism (i.e. ZIPB and pufferfish ZIP2) (28,29). Nevertheless, this does not necessarily hold true for all the ZIP members, as some of them have been postulated to possess different transport mechanisms. For example, ZIP8 and

ZIP14 are described as metal/bicarbonate symporters (47,48). In this regard, as mentioned previously, preliminary experiment from our laboratory, monitoring Cd^{2+}-fluxes through human ZIP8 overexpressing cells, showed that the activity of this transporter is not stimulated by extracellular H^+, indicating a transport mechanism that is different from the herein described for ZIP2. This highlights the need for future studies for each ZIP family member individually, in order to reveal their particular transport mechanisms and to understand their distinctive contributions towards body Zn^{2+} homeostasis.

Acknowledgements

The authors would like to highlight and thank Tamara Locher and Yvonne Amrein for their dedication and technical support. J.P.G. was funded by the Marie Curie Actions International Fellowship Program (IFP) TransCure (www.nccr-transcure.ch).

References

1. Gaither, L. A., and Eide, D. J. (2000) Functional expression of the human hZIP2 zinc transporter. *J Biol Chem* **275**, 5560-5564
2. Franz, M. C., Simonin, A., Graeter, S., Hediger, M. A., and Kovacs, G. (2014) Development of the First Fluorescence Screening Assay for the SLC39A2 Zinc Transporter. *J Biomol Screen* **19**, 909-916
3. Desouki, M. M., Geradts, J., Milon, B., Franklin, R. B., and Costello, L. C. (2007) hZip2 and hZip3 zinc transporters are down regulated in human prostate adenocarcinomatous glands. *Mol Cancer* **6**, 37
4. Inoue, Y., Hasegawa, S., Ban, S., Yamada, T., Date, Y., Mizutani, H., Nakata, S., Tanaka, M., and Hirashima, N. (2014) ZIP2 protein, a zinc transporter, is associated with keratinocyte differentiation. *J Biol Chem* **289**, 21451-21462
5. Tao, Y. T., Huang, Q., Jiang, Y. L., Wang, X. L., Sun, P., Tian, Y., Wu, H. L., Zhang, M., Meng, S. B., Wang, Y. S., Sun, Q., and Zhang, L. Y. (2013) Up-regulation of Slc39A2(Zip2) mRNA in peripheral blood mononuclear cells from patients with pulmonary tuberculosis. *Mol Biol Rep* **40**, 4979-4984
6. Andreini, C., Banci, L., Bertini, I., and Rosato, A. (2006) Counting the zinc-proteins encoded in the human genome. *J Proteome Res* **5**, 196-201
7. Maret, W., and Li, Y. (2009) Coordination dynamics of zinc in proteins. *Chemical reviews* **109**, 4682-4707
8. Brown, K. H., Peerson, J. M., Rivera, J., and Allen, L. H. (2002) Effect of supplemental zinc on the growth and serum zinc concentrations of prepubertal children: a meta-analysis of randomized controlled trials. *Am J Clin Nutr* **75**, 1062-1071
9. Eide, D. J. (2006) Zinc transporters and the cellular trafficking of zinc. *Biochim Biophys Acta* **1763**, 711-722
10. Palmiter, R. D., and Huang, L. (2004) Efflux and compartmentalization of zinc by members of the SLC30 family of solute carriers. *Pflugers Arch* **447**, 744-751
11. Jeong, J., and Eide, D. J. (2013) The SLC39 family of zinc transporters. *Molecular Aspects of Medicine* **34**, 612-619
12. Liuzzi, J. P., and Cousins, R. J. (2004) Mammalian zinc transporters. *Annu Rev Nutr* **24**, 151-172
13. Cao, J., Bobo, J. A., Liuzzi, J. P., and Cousins, R. J. (2001) Effects of intracellular zinc depletion on metallothionein and ZIP2 transporter expression and apoptosis. *J Leukoc Biol* **70**, 559-566

14. Rishi, I., Baidouri, H., Abbasi, J. A., Bullard-Dillard, R., Kajdacsy-Balla, A., Pestaner, J. P., Skacel, M., Tubbs, R., and Bagasra, O. (2003) Prostate cancer in African American men is associated with downregulation of zinc transporters. *Appl Immunohistochem Mol Morphol* **11**, 253-260
15. Franz, M. C., Anderle, P., Bürzle, M., Suzuki, Y., Freeman, M. R., Hediger, M. A., and Kovacs, G. (2013) Zinc transporters in prostate cancer. *Molecular Aspects of Medicine* **34**, 735-741
16. Costello, L. C., Franklin, R. B., Zou, J., Feng, P., Bok, R., Mark, G. S., and Kurhanewicz, J. (2011) Human prostate cancer ZIP1/zinc/citrate genetic/metabolic relationship in the TRAMP prostate cancer animal model. *Cancer Biol Ther* **12**
17. Franklin, R. B., Feng, P., Milon, B., Desouki, M. M., Singh, K. K., Kajdacsy-Balla, A., Bagasra, O., and Costello, L. C. (2005) hZIP1 zinc uptake transporter down regulation and zinc depletion in prostate cancer. *Mol Cancer* **4**, 32
18. Johnson, L. A., Kanak, M. A., Kajdacsy-Balla, A., Pestaner, J. P., and Bagasra, O. (2010) Differential zinc accumulation and expression of human zinc transporter 1 (hZIP1) in prostate glands. *Methods* **52**, 316-321
19. Hara, T., Takeda, T. A., Takagishi, T., Fukue, K., Kambe, T., and Fukada, T. (2017) Physiological roles of zinc transporters: molecular and genetic importance in zinc homeostasis. *J Physiol Sci* **67**, 283-301
20. Montalbetti, N., Simonin, A., Dalghi, M. G., Kovacs, G., and Hediger, M. A. (2014) Development and Validation of a Fast and Homogeneous Cell-Based Fluorescence Screening Assay for Divalent Metal Transporter 1 (DMT1/SLC11A2) Using the FLIPR Tetra. *J Biomol Screen* **19**, 900-908
21. Kovacs, G., Montalbetti, N., Simonin, A., Danko, T., Balazs, B., Zsembery, A., and Hediger, M. A. (2012) Inhibition of the human epithelial calcium channel TRPV6 by 2-aminoethoxydiphenyl borate (2-APB). *Cell Calcium* **52**, 468-480
22. Romero, M. F., Fong, P., Berger, U. V., Hediger, M. A., and Boron, W. F. (1998) Cloning and functional expression of rNBC, an electrogenic Na(+)-HCO3- cotransporter from rat kidney. *Am J Physiol* **274**, F425-432
23. DeGrado, T. R., Pandey, M. K., Byrne, J. F., Engelbrecht, H. P., Jiang, H., Packard, A. B., Thomas, K. A., Jacobson, M. S., Curran, G. L., and Lowe, V. J. (2014) Preparation and preliminary evaluation of 63Zn-zinc citrate as a novel PET imaging biomarker for zinc. *J Nucl Med* **55**, 1348-1354
24. Oyama, Y., Arata, T., Chikahisa, L., Soeda, F., and Takahama, K. (2002) Estimation of increased concentration of intracellular Cd(2+) by fluo-3 in rat thymocytes exposed to CdCl(2). *Environ Toxicol Pharmacol* **11**, 111-118
25. Pujol-Gimenez, J., Hediger, M. A., and Gyimesi, G. (2017) A novel proton transfer mechanism in the SLC11 family of divalent metal ion transporters. *Sci Rep* **7**, 6194
26. Cheng, Y., and Prusoff, W. H. (1973) Relationship between the inhibition constant (K1) and the concentration of inhibitor which causes 50 per cent inhibition (I50) of an enzymatic reaction. *Biochem Pharmacol* **22**, 3099-3108
27. Mackenzie, B., Ujwal, M. L., Chang, M. H., Romero, M. F., and Hediger, M. A. (2006) Divalent metal-ion transporter DMT1 mediates both H+ -coupled Fe2+ transport and uncoupled fluxes. *Pflugers Arch* **451**, 544-558
28. Lin, W., Chai, J., Love, J., and Fu, D. (2010) Selective electrodiffusion of zinc ions in a Zrt-, Irt-like protein, ZIPB. *J Biol Chem* **285**, 39013-39020
29. Qiu, A., and Hogstrand, C. (2005) Functional expression of a low-affinity zinc uptake transporter (FrZIP2) from pufferfish (Takifugu rubripes) in MDCK cells. *Biochem J* **390**, 777-786
30. Chen, M. F., and Chen, T. Y. (2001) Different fast-gate regulation by external Cl(-) and H(+) of the muscle-type ClC chloride channels. *J Gen Physiol* **118**, 23-32
31. Kang, I. S., Cho, J. H., Choi, I. S., Kim, D. Y., and Jang, I. S. (2016) Acidic pH modulation of Na+ channels in trigeminal mesencephalic nucleus neurons. *Neuroreport* **27**, 1274-1280

32. Chauvigne, F., Zapater, C., Stavang, J. A., Taranger, G. L., Cerda, J., and Finn, R. N. (2015) The pH sensitivity of Aqp0 channels in tetraploid and diploid teleosts. *FASEB J* **29**, 2172-2184
33. Holzer, P. (2009) Acid-sensitive ion channels and receptors. *Handb Exp Pharmacol*, 283-332
34. Franz, M. C., Anderle, P., Burzle, M., Suzuki, Y., Freeman, M. R., Hediger, M. A., and Kovacs, G. (2013) Zinc transporters in prostate cancer. *Mol Aspects Med* **34**, 735-741
35. Charalabopoulos, K., Karachalios, G., Baltogiannis, D., Charalabopoulos, A., Giannakopoulos, X., and Sofikitis, N. (2003) Penetration of antimicrobial agents into the prostate. *Chemotherapy* **49**, 269-279
36. Boer, M., Duchnik, E., Maleszka, R., and Marchlewicz, M. (2016) Structural and biophysical characteristics of human skin in maintaining proper epidermal barrier function. *Postepy Dermatol Alergol* **33**, 1-5
37. Dufner-Beattie, J., Langmade, S. J., Wang, F., Eide, D., and Andrews, G. K. (2003) Structure, function, and regulation of a subfamily of mouse zinc transporter genes. *J Biol Chem* **278**, 50142-50150
38. Lane, D. J., Robinson, S. R., Czerwinska, H., and Lawen, A. (2010) A role for Na+/H+ exchangers and intracellular pH in regulating vitamin C-driven electron transport across the plasma membrane. *Biochem J* **428**, 191-200
39. Vigliarolo, T., Zocchi, E., Fresia, C., Booz, V., and Guida, L. (2016) Abscisic acid influx into human nucleated cells occurs through the anion exchanger AE2. *Int J Biochem Cell Biol* **75**, 99-103
40. Lang, K., Wagner, C., Haddad, G., Burnekova, O., and Geibel, J. (2003) Intracellular pH activates membrane-bound Na(+)/H(+) exchanger and vacuolar H(+)-ATPase in human embryonic kidney (HEK) cells. *Cell Physiol Biochem* **13**, 257-262
41. Yabuuchi, H., Tamai, I., Sai, Y., and Tsuji, A. (1998) Possible role of anion exchanger AE2 as the intestinal monocarboxylic acid/anion antiporter. *Pharm Res* **15**, 411-416
42. Sobczak, K., Bangel-Ruland, N., Leier, G., and Weber, W. M. (2010) Endogenous transport systems in the Xenopus laevis oocyte plasma membrane. *Methods* **51**, 183-189
43. Giacconi, R., Muti, E., Malavolta, M., Cardelli, M., Pierpaoli, S., Cipriano, C., Costarelli, L., Tesei, S., Saba, V., and Mocchegiani, E. (2008) A novel Zip2 Gln/Arg/Leu codon 2 polymorphism is associated with carotid artery disease in aging. *Rejuvenation Res* **11**, 297-300
44. Karagas, M. R., Andrew, A. S., Nelson, H. H., Li, Z., Punshon, T., Schned, A., Marsit, C. J., Morris, J. S., Moore, J. H., Tyler, A. L., Gilbert-Diamond, D., Guerinot, M. L., and Kelsey, K. T. (2012) SLC39A2 and FSIP1 polymorphisms as potential modifiers of arsenic-related bladder cancer. *Hum Genet* **131**, 453-461
45. Kamei, S., Fujikawa, H., Nohara, H., Ueno-Shuto, K., Maruta, K., Nakashima, R., Kawakami, T., Matsumoto, C., Sakaguchi, Y., Ono, T., Suico, M. A., Boucher, R. C., Gruenert, D. C., Takeo, T., Nakagata, N., Li, J. D., Kai, H., and Shuto, T. (2018) Zinc Deficiency via a Splice Switch in Zinc Importer ZIP2/SLC39A2 Causes Cystic Fibrosis-Associated MUC5AC Hypersecretion in Airway Epithelial Cells. *EBioMedicine* **27**, 304-316
46. Hamon, R., Homan, C. C., Tran, H. B., Mukaro, V. R., Lester, S. E., Roscioli, E., Bosco, M. D., Murgia, C. M., Ackland, M. L., Jersmann, H. P., Lang, C., Zalewski, P. D., and Hodge, S. J. (2014) Zinc and zinc transporters in macrophages and their roles in efferocytosis in COPD. *PLoS One* **9**, e110056
47. Girijashanker, K., He, L., Soleimani, M., Reed, J. M., Li, H., Liu, Z., Wang, B., Dalton, T. P., and Nebert, D. W. (2008) Slc39a14 gene encodes ZIP14, a metal/bicarbonate symporter: similarities to the ZIP8 transporter. *Mol Pharmacol* **73**, 1413-1423
48. He, L., Girijashanker, K., Dalton, T. P., Reed, J., Li, H., Soleimani, M., and Nebert, D. W. (2006) ZIP8, member of the solute-carrier-39 (SLC39) metal-transporter family: characterization of transporter properties. *Mol Pharmacol* **70**, 171-180

For Table of contents use only